



VICTORIA UNIVERSITY
MELBOURNE AUSTRALIA

A Circuit Model of Real Time Human Body Hydration

This is the Accepted version of the following publication

Asogwa, Clement, Teshome, Assefa, Collins, Stephen F and Lai, Daniel (2015)
A Circuit Model of Real Time Human Body Hydration. IEEE Transactions on
Biomedical Engineering, 63 (6). pp. 1239-1247. ISSN 0018-9294

The publisher's official version can be found at
<https://ieeexplore.ieee.org/document/7299616>
Note that access to this version may require subscription.

Downloaded from VU Research Repository <https://vuir.vu.edu.au/30125/>

A Circuit Model of Real Time Human Body Hydration

Clement Ogugua Asogwa, *Student Member, IEEE*,

Assefa K. Teshome, *Member, IEEE*, Stephen F. Collins, and Daniel T.H. Lai, *Member, IEEE*.

Abstract—Changes in human body hydration leading to excess fluid losses or overload affects the body fluid’s ability to provide the necessary support for healthy living. We propose a time dependent circuit model of real time human body hydration, which models the human body tissue as a signal transmission medium. The circuit model predicts the attenuation of a propagating electrical signal. Hydration rates are modelled by a time constant τ which characterises the individual specific metabolic function of the body part measured. We define a surrogate human body anthropometric parameter θ by the muscle-fat ratio and comparing it with the Body Mass Index (BMI), we find theoretically, the rate of hydration varying from 1.73 dB/minute, for high θ and low τ to 0.05 dB/minute for low θ and high τ . We compare these theoretical values with empirical measurements and show that real time changes in human body hydration can be observed by measuring signal attenuation. We took empirical measurements using a vector network analyser and obtained different hydration rates for various BMI, ranging from 0.6 dB/minute for 22.7 kg/m² down to 0.04 dB/minute for 41.2 kg/m². We conclude that the galvanic coupling circuit model can predict changes in the volume of the body fluid which are essential in diagnosing and monitoring treatment of body fluid disorder. Individuals with high BMI would have higher time-dependent biological characteristic, lower metabolic rate and lower rate of hydration.

Index Terms—Galvanic Coupling, Signal propagation, Attenuation, Hydration, Metabolic rate and BMI.

I. INTRODUCTION

STUDIES in human body composition are essential because it is linked to the risks of unhealthy states of the body. For example, changes in fluid levels in the body can affect its ability to provide the necessary support for healthy living[1]. Conditions leading to excess fluid losses in the body usually result in problems such as dehydration, while fluid overload can lead to heart failure and death in some cases [2]. Hydration in this context is defined as the process of gaining tissue water and the rate of hydration as the amount of change in the level of tissue water with respect to time. Hydration measurements are used to determine the amount of fluid in the body and as a symptom for diseases associated with excess fluid or low level fluid in a human body [3]. Two major techniques for

measuring total body hydration are bioelectrical impedance analysis [4] and urine specific gravity [5][6]. These techniques assume a constant hydration factor and cannot be applied to a specific area of the body. For instance, the bioelectrical impedance analysis method is based on a hypothetical relationship between impedance and the electrical volume. It assumes that the entire human body is a cylindrical conductor and tissues are electrically isotropic with no reactance component. However, it has been shown that human tissue should be modelled as having both resistive and reactive components since cell membrane capacitance contributes significantly to the effective impedance of electrical signals across tissues [7]. Schwan further showed that biological tissues have frequency dependent electrical properties that could classify them into three frequency regions (α, β, γ)[8]. Current treatment of body fluid disorders such as lymphoedema are mostly monitored by changes in body weight, circumferential limb measurements, limb volume measurements, and water displacement methods which have issues with hygiene and problems with tracking sequential changes in weight and limb circumference [9]. A new method is required to measure body fluid levels effectively.

We propose a circuit model that models tissue layers as an electrical network with capacitive and resistive components. The resulting circuit model has a transfer function that describes the signal attenuation (negative gain) when an electrical signal is galvanically transmitted through the human body. These attenuations can be measured allowing us to quantify hydration effects empirically and hygienically while tracking changes in the fluid volume on a specific area of the body.

A. Signal Propagation Through The Human Tissue

Electrical signal propagation across tissues are influenced by frequency-dependent dielectric properties of tissues. These are primarily affected by the extracellular and the intracellular fluids in the body. Fig.1 and Fig.2 depict the dielectric relationship with frequency of common human tissues. The high relative permittivity at lower frequencies implies that signal propagation across human tissues would have higher attenuation which we shall use for our investigation. Since relative permittivity of tissue is higher at low frequencies (Fig.2), we propose observing signal attenuation on tissues at low frequencies to measure variabilities in human body hydration with respect to time. In addition high frequencies are affected by external factors such as the human body antenna effect and possible radiation. Our frequency range lies within

Clement Ogugua Asogwa is a research student at the College of Engineering and Science, Victoria University, Melbourne, Australia(e-mail: clement.asogwa@live.vu.edu.au)

Assefa K. Teshome, Stephen F. Collins and Daniel T.H. Lai are with Victoria University, College of Engineering and Science, Victoria University, Melbourne, Australia.

Copyright (c) 2015 IEEE. Personal use of this material is permitted. However, permission to use this material for any other purposes must be obtained from the IEEE by sending an email to pubs-permissions@ieee.org.

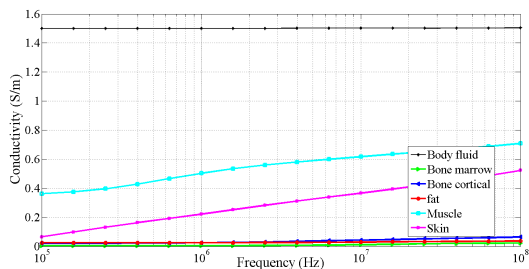


Fig. 1. Conductivity (S/m) of tissues at different frequencies. Data source [17]

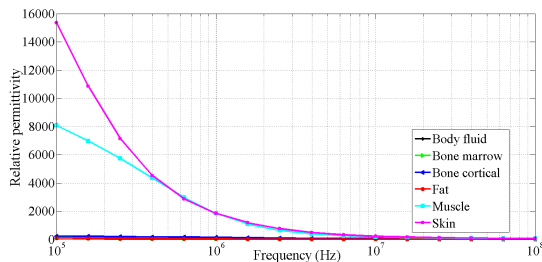


Fig. 2. Relative permittivity of tissues at different frequencies. Data source [17]

the β dispersion region [8] which is related to the cellular structure of biological materials. At higher frequencies, dipolar reorientation of proteins and organelles can occur which is not favourable. To the best of our knowledge, previous models of signal propagation across the human tissue, either by finite-element method [10-11], finite difference time-domain methods [12], equivalent electric circuit [13-14] and quasi-static dielectric principles [15] are all based on the assumption of static tissue impedance. This assumption is less accurate considering that the average quantity of water consumed by a normal person to replace lost fluid in a temperate environment is between 2600 - 2700 ml per day [16]. These dynamic changes in the body fluid level, which also changes the impedance of the body, and the high relative permittivity at low frequencies is our motivation for a real-time human body circuit model to describe human body hydration.

The rest of the paper is organised as follows: In section II we propose a first-order model of human body hydration with a mathematical expression of the transfer function derived from our circuit model containing a time varying impedance component. In section III we present our experimental set-up for the empirical measurements and in section IV the results. Finally, the paper concludes with the discussion in section V and the conclusion in section VI.

II. HYDRATION MODEL

A. Previous Circuit Model of The Human Body

In previous work, Wegmueller et al. [18] proposed a four-terminal circuit model with five body tissue impedances (Fig.3), which was later improved by Song et al [13] and most recently by our group [14]. Our previous model included Z_{ES} representing the impedance of the contact interface to the

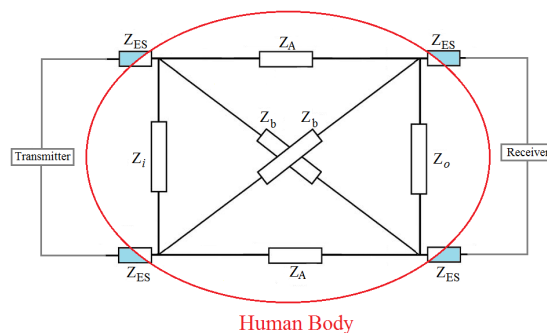


Fig. 3. Simplified four terminal galvanically coupled IBC circuit showing approximations of the impedance components [18]

body at the transmitter and the receiver nodes, Z_i and Z_o are the input and output impedances which corresponds to the transverse impedance Z_T . Z_A is the longitudinal impedance of the transmission path corresponding to Z_L in (Fig.4). The impedance Z_L in our previous model consisted of the skin, fat, muscle, and bone, which we have extended to six layers by including a body fluid layer and the cortical bone and bone marrow because the cortical bone and bone marrow have different dielectric properties [7].

B. Proposed Model of Hydration as a Time Dependent Circuit

We propose a variable impedance component $Z_F(t)$ (Fig.4) that changes with a change in volume of the body fluid. The body fluid increases or decreases primarily by hydration or dehydration. We assume an average arm radius of 50 mm. The corresponding tissues consist of 3% skin, 17% fat, 55% muscle, 12% cortical bone, and 13% bone marrow [19]. We used these to calculate the tissue anthropometric parameters (the thickness of the tissue layers at different arm radii), then by optimization, we calculated the corresponding amount of the thickness of the body fluid layer. However, although body parts have multifaceted geometry with complex internal structures, we assume a homogeneous concentration of these proportions including a fluid layer over the entire arm. We calculated the impedance of the six body tissue components in this model using the formula in [13] since our previous model assumed negligible diagonal impedance Z_b (Fig.4) and like other circuit models did not consider the effect of the dynamic changes in the body fluid.

We postulate that the changes in the amount of water in the body directly changes the resultant impedance of the body tissues which causes an increase or decrease in the received signal attenuation. The body fluid consists mainly of aqueous solutions of ions and cations which influence the signal propagation [7].

C. Estimation of the Fluid Component of the Arm

The effects of hydration changes have not been taken into account in human body circuit models. To introduce the variable fluid component, we have an approximation of a separate fluid layer among the tissues using Fig.5, Fig.6 and table II. Water contributes up to 60% of total body weight

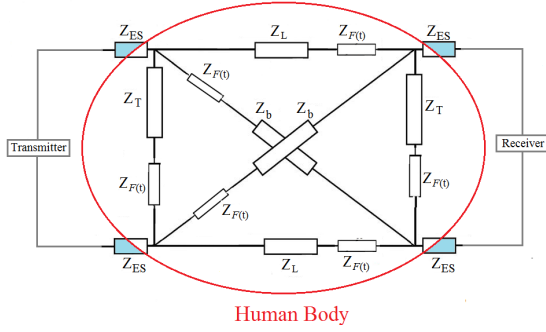


Fig. 4. Improved circuit with variable impedance component from dynamic changes in human body fluid volume

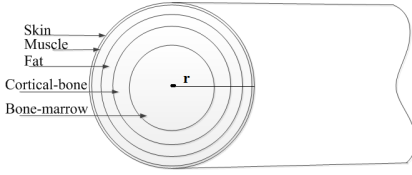


Fig. 5. The cross section of the arm with radius r , showing the different tissue layers used in our simulation experiment

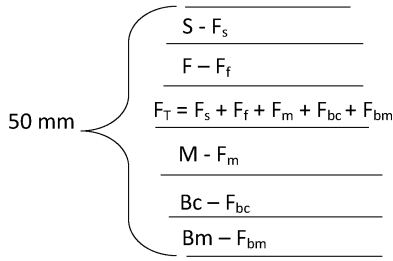


Fig. 6. Approximating the fluid layer by optimization

(TBW) of an adult [1]. The dipole nature of water results in ions which contribute to electrolytic conductivity [7]. Table 1 shows some of the human body electrolytes.

TABLE I
EXAMPLE OF BODY ELECTROLYTES [7]

Cations	Anions
Na^+	Cl^-
K^+	HCO_3^-
Ca^{2+}	$Protein^-$
Mg^{2+}	PO_4^{2-}
H^+	SO_4^{2-}

Both the intracellular and the extracellular electrolytes support electrolytic conductivity which causes potential differences that influence current flow. The conductivity is related to the movement of the electrolytes; adipose tissues contain relatively less water than muscle tissues causing conductivity to be less in fat than in muscle and skin [7]. To estimate the body fluid we assume a non-homogeneous lower arm with a homogeneous distribution of the fluid.

Let F_n denote the thickness of fluid in the n th layer of the arm, consisting of the skin s , fat f , muscle m , cortical bone

bc and bone marrow bm ; therefore, the thickness of the fluid layer, F_T would be

$$F_T = F_s + F_f + F_m + F_{bc} + F_{bm} \quad (1)$$

As depicted in Fig.6, each layer includes a fluid layer F with subscript as shown in equation 1. Similarly, if r is radius of the arm [18] and t_n the thickness of the n th layer of the arm from skin, fat, muscle, body fluid, bone cortical and bone marrow, the cross sectional area of first layer with arm radius $r = 50mm$ would be

$$\pi(r^2 - (50 - t_1)^2) \quad (2)$$

while the other layers would be

$$\pi((50 - t_{n-1})^2 - (50 - t_{n-1} - t_n)^2) \quad (3)$$

TABLE II
PERCENTAGE OF WATER ON BODY TISSUES [1, 20]

Tissue Type	Percentage of Water	Thickness on arm radius (50 mm)
Skin	44	3
Fat	10	17
Muscle	70	55
Bone	22	a) Cortical bone 12 b) Bone Marrow 13

From table II and Fig.6 and computing with equations 1-3, we have the total thickness of the fluid layer F_T to be approximately 23 mm.

D. First-Order Model of The Changes in Human Body Impedance As a Result of Hydration

Based on Fig.4 the transfer function can be derived. Since the circuit is symmetrical, we have that the new circuit would have a variable impedance component $Z_F(t)$ in both the transverse and longitudinal sides, Z_T and Z_L respectively. V_i is the transmit voltage while V_0 is the output voltage at the receiver end with load R_l . Therefore, we infer that any dynamic change in the impedance caused by a change in the human body hydration state would result in a change of the impedance of Z_T , Z_L , and Z_b as following:

$$\dot{Z}_T = Z_T + Z_F(t) \quad (4)$$

$$\dot{Z}_L = Z_L + Z_F(t) \quad (5)$$

$$\dot{Z}_b = Z_b + Z_F(t) \quad (6)$$

$$V_0 = I_0 R_l = \frac{V_i R_l \sigma_5}{\sigma_2} \quad (7)$$

Hence, the circuit model from Fig.15 is

$$\frac{V_0}{V_i} = \frac{-R_l \sigma_5}{\sigma_2} = \frac{-2R_l \dot{Z}_T^2 (\dot{Z}_b + \dot{Z}_L)}{\sigma_2} \quad (8)$$

where $\sigma_2 =$

$$8Z_{ES}^2 (\dot{Z}_L^2 + \dot{Z}_L \dot{Z}_T + \dot{Z}_b \dot{Z}_L + \dot{Z}_b \dot{Z}_T) + 4Z_{ES} \dot{Z}_L^2 (\dot{Z}_L + \dot{Z}_T + \dot{Z}_b) + 4Z_{ES} \dot{Z}_T (\dot{Z}_L \dot{Z}_T + \dot{Z}_b \dot{Z}_L + \dot{Z}_b \dot{Z}_T) + 2\dot{Z}_L^2 \dot{Z}_T (\dot{Z}_L + \dot{Z}_b);$$

$$\text{and } \sigma_5 = 2\dot{Z}_b\dot{Z}_T^2 + 2\dot{Z}_L\dot{Z}_T^2;$$

The details of the derivation can be found in Appendix A.

We propose that a measurable change in the amount of body fluid will result in a change in a time-dependent impedance element $Z_F(t)$ for time t after fluid intake and hydration occurs. This means that the transfer function (equation 8) is also time-dependent i.e

$$\frac{V_0}{V_i} = g(t) \quad (9)$$

And the signal gain

$$G = 20\log\frac{V_0}{V_i} \quad (10)$$

also varies proportionally with the time-varying changes in the impedance of the body as a result of the changes in the body fluid volume.

After fluid intake, as hydration occurs, the impedance of the body fluid $Z_F(t)$ decreases. This causes a decrease in the signal attenuation of the electrical signal passing through the tissues. If we denote the initial state of the impedance at $t = 0$ just before hydration as Z_{f0} , we propose that as the body fluid increases, the time-dependent impedance of the body fluid decreases in the form of a first order process given by

$$Z_F(t) = Z_{f0} - Z_w(1 - e^{-\frac{t}{\tau}}) \quad (11)$$

where t is the time for the change in impedance to occur, Z_{f0} is the impedance at time $t = 0$ just before hydration begins, t_f is time to reach the state of water balance, Z_w is the impedance resulting from the water consumed and the ratio $\frac{t}{\tau}$ is a characteristic that predicts the rate of hydration. τ is the time constant that characterises a particular individual. Therefore, assuming an initial fluid volume V_{ib} before hydration, V_w is the amount of fluid consumed then the body will hydrate to a fluid volume V_b given as

$$V_b = V_{ib} + V_w e^{\frac{t}{\tau}}; t = 0; V_b = V_{ib} \quad (12)$$

We propose equation (12) as the formula for estimating human body hydration at time t after fluid intake. V_w is the amount of water consumed by the subject, t is the time to absorb $V_w e^{\frac{t}{\tau}}$ amount of water. Fig.7 shows the effects of τ on the rate of hydration.

To verify the effects of the anthropometric measurements, we propose θ to denote the muscle-fat ratio as a surrogate measure of body fat, similar in definition to the body mass index, BMI measured in (kg/m^2) [21]. We set the dimensions of the tissues contributing to the longitudinal impedance to the distance between the transmitter and receiver electrode pairs and use the cross-sectional area of muscle and fat to calculate θ as

$$\theta = \frac{A_m}{A_f} \quad (13)$$

$$= \frac{\pi(r^2 - (50 - (t_1 + t_2 + t_3 + t_4))^2)}{\pi(r^2 - (50 - (t_1 + t_2))^2)} \quad (14)$$

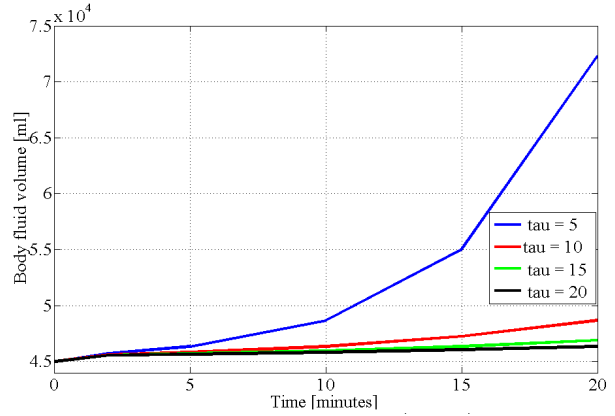


Fig. 7. The effect of τ on the rate of hydration with initial body fluid volume set at 45,000 ml and 500 ml water intake.

A_m is the cross-sectional area of muscle to the distance between the transmitting and receiving electrodes and A_f the cross-sectional area of fat to the same distance between the transmitting and receiving electrode pairs. $t_1 - t_4$ is the thickness of the tissue layers in the arm corresponding to the skin, fat, fluid and muscle layers respectively (Fig.6). Table III is our classification of the anthropometric measurements to represent different indices of the proportion of body fat, by varying the proportions of A_m and f_m in (14), where for the purposes of our simulation $0 < \theta < 1$. We define our anthropometric ratios as high θ corresponding to low fat index or low BMI and low θ corresponding to high fat index or high BMI.

TABLE III
ANTHROPOMETRIC MEASUREMENT INDEX, MUSCLE-FAT RATIO

Index	Ratio
θ_1	0.9
θ_2	0.6
θ_3	0.3
θ_4	0.2

Based on the discussions above, we propose a new expression for signal attenuation (G), in a galvanic coupled human body circuit as $G(f, t, \tau, \theta)$, where f is the input signal frequency, t is the real time of observation, τ is specific to time varying characteristic of the subject, and θ is the anthropometric measurements of the body. The changes in attenuation (negative gain) can be calculated from equation 8

$$G(f, t, \tau, \theta) = 20\log\left(\frac{-2R_i\dot{Z}_T^2(\dot{Z}_b + \dot{Z}_L)}{\sigma_2}\right) \quad (15)$$

where τ is found by equating the measured attenuation to the transfer function equation (15). Fig.8 depicts the effect of different values of τ on the rate of hydration at constant θ while Fig.9 shows the graph corresponding to different proportions of τ and θ that represent different combinations of the individual biological characteristic τ and the anthropometric

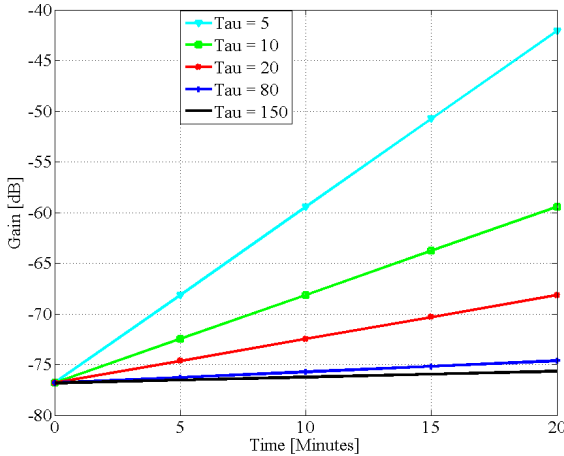


Fig. 8. Graph of attenuation versus time at 800 kHz, showing the effect of changes in τ , at $\theta = 0.9$.

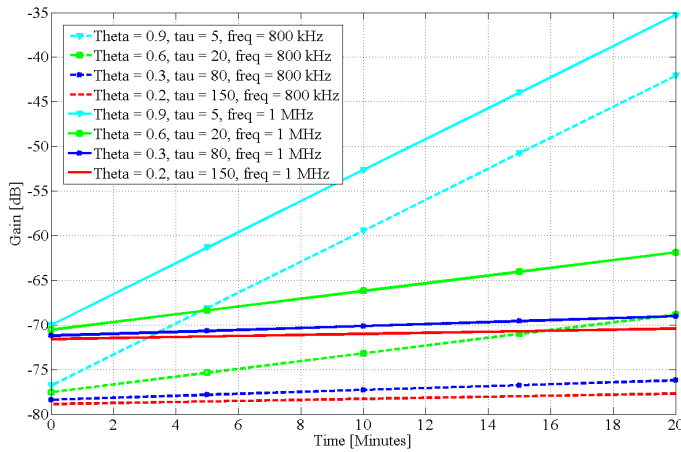


Fig. 9. Model predictions of attenuation for simulated hydration at 800 kHz and 1 MHz when τ is inversely proportional to θ . This indicates low BMI equals lower time-dependent metabolic rate [24], higher rate of hydration [25] and more body of water [27]

ratio θ . Again, we show in Fig.10 is the converse combination of the individual biological characteristic τ and anthropometric ratio θ . Fig.11 is the simulated graph of gain against frequency on an individual with physiological combination of τ and θ .

III. EXPERIMENTAL SET-UP

A. Determination of the variability of fluid impedance with changes in the volume of water

The measurement set-up is as shown in Fig.17. A mini Pro VNA, frequency range 100 kHz to 200 MHz, manufactured by Mini Radio Solutions, baluns (Coaxial RF transformers, FTB-1-1+, turns ratio of one, manufactured by Mini-Circuits, and frequency range 0.2-500 MHz), and round pre-gelled

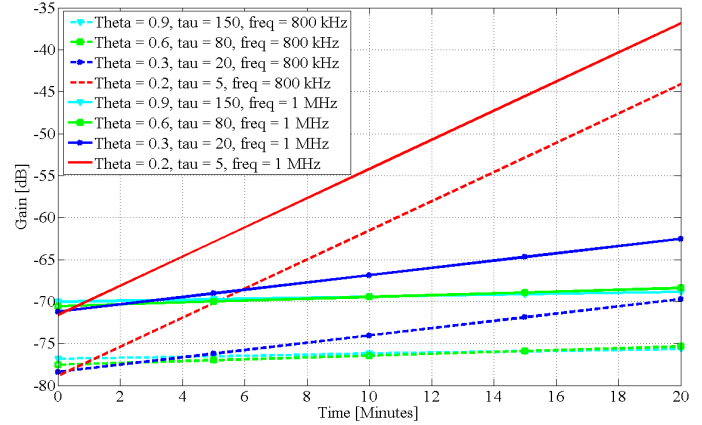


Fig. 10. Model predictions of attenuation for simulated hydration at 800 kHz and 1 MHz where τ is proportional to θ . The result shows high BMI has high hydration rate and low time-dependent metabolic rate. This is not supported by empirical results and is not explained physiologically

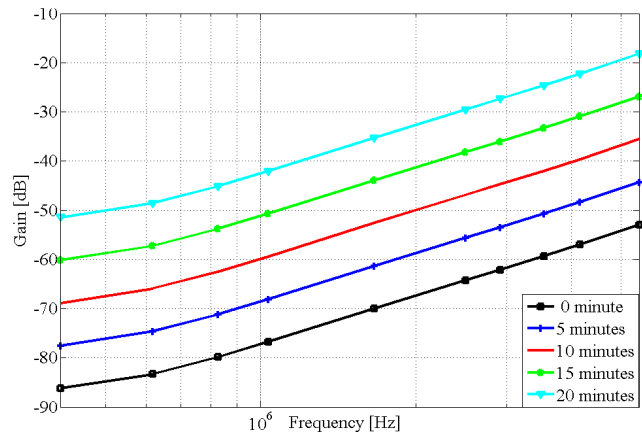


Fig. 11. Attenuation against frequency as hydration occurs with $\tau = 5$ and $\theta = 0.9$.

self-adhesive Ag/AgCl snap single electrodes (1 cm diameter, manufactured by Noraxon) were used. The baluns were used to electrically isolate the two ports of the VNA to ensure the return current does not pass through the common earth ground of the two ports. The VNA is set to sweep the constant interval frequency of range 300 kHz to 5.4 MHz in 49 points with 0 dBm output power. This is well below the safety limit set by International Commission on Non-Ionizing Radiation Protection (ICNIRP, 1998) and World Health Organization (WHO, 1993) [22]. The Noraxon self-adhesive Silver/Silver-Chloride electrodes (Ag/AgCl) are preferred because it reduces the effects of motion artifacts and reflection. The distance between the transmit and receive electrodes and the inter

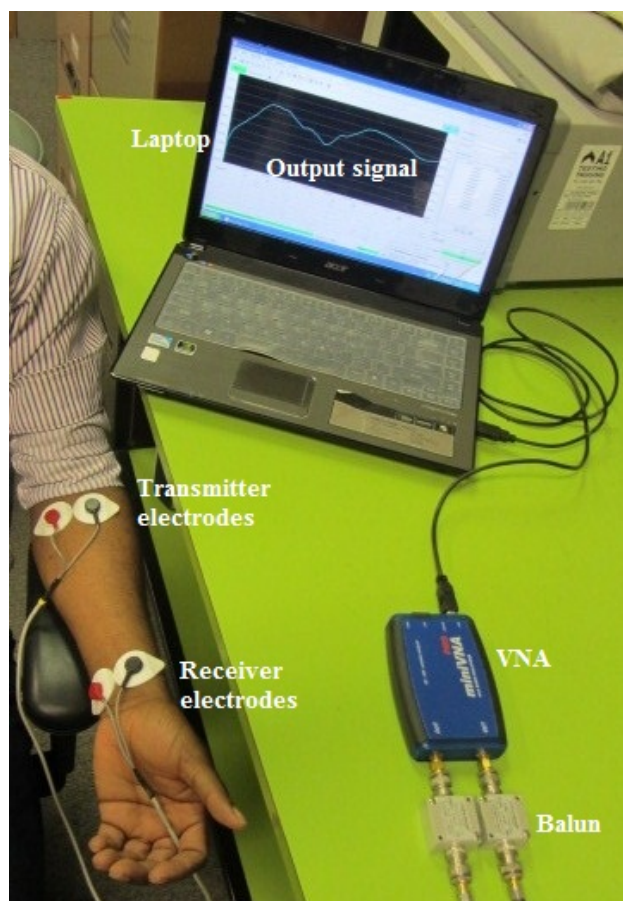


Fig. 12. Galvanic-coupling circuit on the lower left arm, the four terminal silver-silver chloride surface electrodes are attached to the body and connected to the VNA via a balun. The output signal shows on the laptop screen fitted with the VNA software

electrode separation is 20 cm and 4 cm respectively. A small harmless electrical current (<1 mA) is transmitted into the arm via a pair of Noraxon surface electrodes (transmitter electrodes) and received 20 cm at the receiver end as shown in Fig.12. Six healthy volunteers participated in the experiment. First the subjects were asked to abstain from fluid after supper to 10.00 am. The subjects were given 500 ml of water and measured separately after fluid intake. All the subjects sat on a plastic chair with arms by the side to ensure the current was confined within the arm and avoiding external physical contact. Since individual metabolism is different at different times of the day, our experimental protocol was designed to ensure that all measurements were done at 10.00 am and that the average room temperature was maintained at $25 \pm 0.1^\circ\text{C}$. Repeated measurements were taken after abstinence from fluid and at 5 minutes interval following fluid intake of 500 ml of water and the average used to minimise measurement uncertainties. Subjects followed ethics procedures mandated by the Victoria University Human Ethics Research Committee.

IV. RESULTS

The theoretical graphs show different rates of hydration as a result of time-varying changes in the impedance of the body and the effects of the changes in τ . Based on our model, we

are proposing to measure the rate of hydration by changes in signal attenuation in dB/minute. From Fig.8, the rate of hydration is 1.73 dB/minute when τ is 5 and 0.05 dB/minute when τ is 150. the graph shows that low τ is associated with high rate of hydration and high τ with low rate of hydration. Fig.9 is our model prediction of attenuation as hydration occurs at 800 kHz and 1 MHz. At state 0, just before hydration begins, signal gain at 800 kHz for $\theta = 0.2$ and $\tau = 150$ is -78.0 dB. This is about 6 dB difference with subject A, BMI 20.1 at 800 kHz and about 8.0 dB difference with subject F, BMI 41.2. Similar observation was also made at 1 MHz. Our combinations of θ and τ is based on our earlier definition of θ as being related to BMI and τ as related to specific individual metabolic processes and since small values of τ resulted in higher rates of hydration, we therefore relate high θ to low τ and low θ to high τ as shown in Figs.8-9. This means that individuals with low anthropometric ratios θ are predicted to have low hydration rates while high θ would have higher rate of hydration. Fig.10 shows the converse combination of τ as proportional to θ which does not match our empirical results at both 800 kHz and 1 MHz. Fig.11 shows that attenuation is affected by time across each frequency. Further comparison of the empirical graphs (Figs.13-14) with the theoretical simulations show that in both cases, all the subjects showed that signal attenuation decreases as the body hydrates, in line with our theoretical prediction (Fig.10). This means that the human body impedance varies with time as the fluid level changes. Again, the six subjects have different anthropometric ratios defined by their BMI which contributed to the individual rate of hydration. Subjects A, B and C have higher rates of hydration and lower BMI ranges. For example, subject B (BMI 22.7) has average rate of hydration as 0.6 dB/minute and 0.7 dB/minute at 800 kHz and 1 MHz respectively. Similarly, subjects with high BMI (D, E and F) have almost a flat rate of hydration corresponding to their low anthropometric values as predicted by our theoretical definition. The decrease in attenuation is across all the subjects and at different rates, characterised by their differences in τ and θ , have been predicted by our simulation results. A comparison of the theoretical anthropometric parameters and the BMI ratios of the body show high BMI corresponding to low θ and longer time dependent characteristic factor τ , while low BMI corresponds to high θ with a corresponding low τ .

V. DISCUSSION

In this paper we proposed a time-dependent impedance circuit model of real-time human body hydration and found that similar to our theoretical predictions, the attenuation of an electrical signal passing through the body tissues changes as the fluid level changes. This change is affected by external factors such as changes in atmospheric temperature, which was minimised in our experiment, as well as individual anthropometric ratio and metabolic rates. The human body regulates the movement of water between the intracellular and the extracellular tissue spaces to maintain effective osmolarity of solutes within each compartment and to maintain a state of water balance. These dynamic variations underline a constant

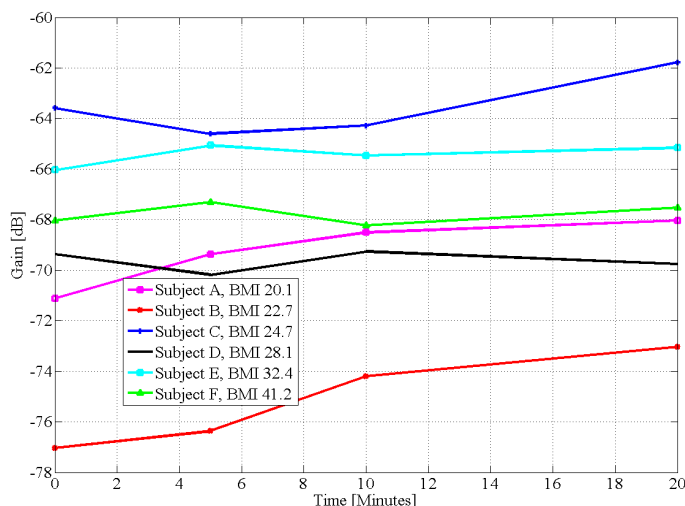


Fig. 13. Changes in signal gain at 800 kHz as hydration occurs on 6 subjects after fluid intake

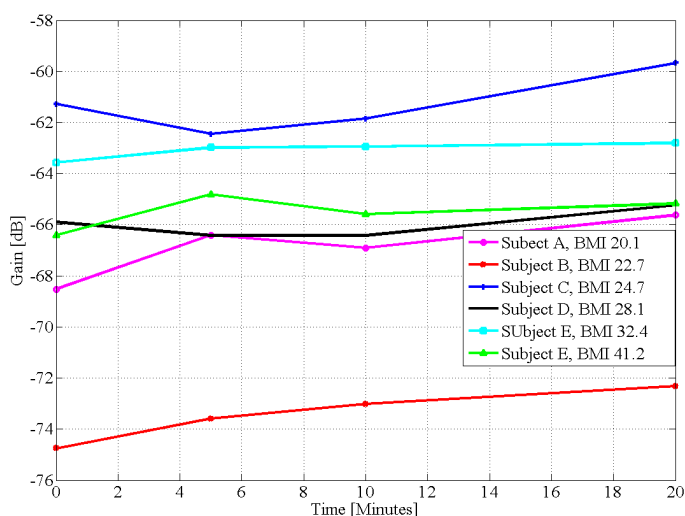


Fig. 14. Changes in signal gain at 1 MHz as hydration occurs on 6 subjects after fluid intake

and varying change in the body impedance as the fluid level changes. A further water intake above obligatory water loss, in a healthy person, is usually excreted in dilute urine [23]. Hence, fluid intake after the state of water balance is reached does not cause hydration. Also fluid absorption rates varies per individual and peak rates are reached at different times.

This study presents a model for evaluating human body hydration by measuring the changes in electrical signal attenuation as it propagates across tissues. We modelled a time-dependent circuit of the body tissues that captures the fluid changes resulting from hydration. We proposed a time constant τ which represented the dynamic metabolic activities of an individual that affects the body hydration rate. We found that smaller values of τ are associated with higher rates of hydration and larger values of τ with lower rates of hydration

(Fig.8). Since τ is representative of the time for complex processes of an individual metabolism, our observation on τ (Fig.8) coincides with Webb's findings [24] that subjects with lower fat free mass have higher time-dependent metabolic characteristic. This is exhibited in Fig.9 for example where τ is inversely proportional to θ and attenuation increases if the proportion of fat increases and decreases if the proportion of fat decreases. Our investigation of the rate of change in attenuation at two separate frequencies 800 kHz and 1 MHz (Fig.9) showed that when θ is 0.9 and τ is 5 the rate of hydration denoted by the rate of change in attenuation is 1.7 dB/minute and when θ is 0.6 and τ is 20 the rate of hydration is 0.5 dB/minute. At $\theta = 0.2$ and $\tau = 150$, the rate of hydration is slower. This matches physiological expectations where lower fat has higher rate of hydration [25]. Fig.10 is the converse prediction of attenuation when τ is proportional to θ . At both 800 kHz and 1 MHz the result is not supported by empirical graphs (Figs. 13-14) and not explained physiologically. Therefore, our parameter θ is related to BMI and BMI is known to be related to metabolic rate. For example, the Mifflin-St. Jeor equation [26] for resting metabolic rate (RMR) shows that metabolic rate is highly proportional to BMI. This means that θ and τ are interrelated.

Our empirical measurements confirm this conjecture and follows the trend predicted by our theoretical model in Fig.9 where τ is inversely related to muscle-fat ratio, θ . Since θ is BMI related, we can then conclude that τ is related to RMR. Indeed, our empirical results show subjects with higher BMI (low θ) having lower hydration rates (high τ) and lower BMI (high θ) having higher rate of hydration (low τ). This also matches physiological expectations that High BMI (low θ) is associated with a higher proportion of fat and smaller body of water [27]. Thus the theoretical hydration patterns of people with different body mass indices in our model (Fig.9 and Fig.11) are supported by the empirical measurements (Figs.13-14). We conclude that under similar conditions and healthy states, individuals with high BMI would have longer time-dependent metabolic process τ , and lower rate of hydration than persons with low BMI. While θ is a measure of the muscle-fat ratio, τ is a complicated mixture of human body metabolic processes which affects hydration.

VI. CONCLUSION

This study presents a new method of measuring the rate of hydration in real time by measuring the changes in the amplitude of a galvanically coupled signal passing through body tissue. We show that real-time changes in signal attenuation can be predicted by a circuit model which incorporates the rate of hydration τ , and human anthropometric measures. Our model will potentially assist in the development of new body fluid monitoring technologies which are essential for diagnosing fluid disorders and a tool for studying fluid requirements in the body. However, a wider experiment is required to determine an explicit model of τ and to determine the effects of other parameters of the body such as age, sex and height.

APPENDIX A
TRANSFER FUNCTION EQUATION

Considering the current flow diagram, using KVL:

$$V_i = 2I_1 Z_{ES} + I_2 \dot{Z}_T \quad (16)$$

$$I_4 \dot{Z}_L = I_2 \dot{Z}_T + I_5 \dot{Z}_b \quad (17)$$

$$I_2 \dot{Z}_T + I_6 \dot{Z}_L = I_4 \dot{Z}_L + I_7 \dot{Z}_T \quad (18)$$

$$I_6 \dot{Z}_L = I_5 \dot{Z}_b + I_7 \dot{Z}_T \quad (19)$$

$$I_4 \dot{Z}_L + I_7 \dot{Z}_T = I_3 \dot{Z}_b \quad (20)$$

$$I_7 \dot{Z}_T = I_8 (2Z_{ES} + \dot{Z}_L) \quad (21)$$

From KCL:

$$I_1 = I_2 + I_3 + I_4 \quad (22)$$

$$I_2 = I_1 + I_5 + I_6 \quad (23)$$

$$I_4 = -I_5 + I_7 + I_8 \quad (24)$$

$$-I_3 = I_7 + I_6 + I_8 \quad (25)$$

$$V_i = 2I_1 Z_{ES} + \dot{Z}_T I_2 + 0 + 0 + 0 + 0 + 0 + 0 \quad (26)$$

$$0 = 0 + I_2 \dot{Z}_T + 0 - \dot{Z}_L I_4 + I_5 \dot{Z}_b + 0 + 0 + 0 \quad (27)$$

$$0 = 0 + 0 + 0 + 0 + I_5 \dot{Z}_b - \dot{Z}_L I_6 + I_7 \dot{Z}_T + 0 \quad (28)$$

$$0 = 0 + 0 - I_3 \dot{Z}_b + I_4 \dot{Z}_L + 0 + 0 + I_7 \dot{Z}_T + 0 \quad (29)$$

$$0 = -I_1 + I_2 + I_3 + I_4 + 0 + 0 + 0 + 0 \quad (30)$$

$$0 = I_1 - I_2 + 0 + 0 + I_5 + I_6 + 0 + 0 \quad (31)$$

$$0 = 0 + 0 + 0 - I_4 - I_5 + 0 + I_7 + I_8 \quad (32)$$

$$0 = 0 + 0 + 0 + 0 + 0 + 0 + -I_7 \dot{Z}_T + (2Z_{ES} + \dot{Z}_L) I_8 \quad (33)$$

The corresponding matrix from the above equations is

$$\begin{bmatrix} V_i \\ 0 \\ 0 \\ 0 \\ 0 \\ 0 \\ 0 \\ 0 \\ 0 \end{bmatrix} =$$

$$\begin{bmatrix} 2Z_{ES} & \dot{Z}_T & 0 & 0 & 0 & 0 & 0 & 0 & 0 \\ 0 & \dot{Z}_T & 0 & -\dot{Z}_L & \dot{Z}_b & 0 & 0 & 0 & 0 \\ 0 & 0 & 0 & 0 & \dot{Z}_b & -\dot{Z}_L & -\dot{Z}_T & 0 & 0 \\ 0 & 0 & -\dot{Z}_b & \dot{Z}_L & 0 & 0 & 0 & \dot{Z}_T & 0 \\ -1 & 1 & 1 & 1 & 0 & 0 & 0 & 0 & 0 \\ 1 & -1 & 0 & 0 & 1 & 1 & 0 & 0 & 0 \\ 0 & 0 & 0 & -1 & -1 & 0 & 1 & 1 & 1 \\ 0 & 0 & 0 & 0 & 0 & 0 & -\dot{Z}_T & 2Z_{ES} + \dot{Z}_L & 0 \end{bmatrix} \begin{bmatrix} I_1 \\ I_2 \\ I_3 \\ I_4 \\ I_5 \\ I_6 \\ I_7 \\ I_8 \end{bmatrix}$$

Solving for I from the above equations

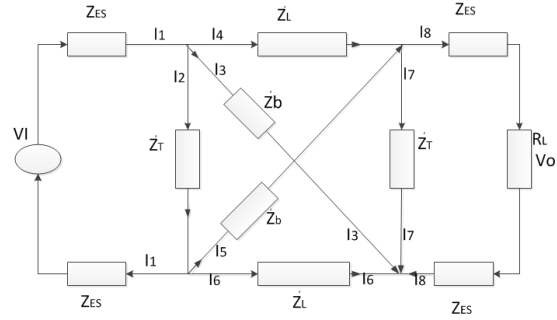


Fig. 15. The equivalent circuit showing directions of the current flow

$$I = \begin{bmatrix} \frac{V_i(2\dot{Z}_b \dot{Z}_T \sigma_0) + 2\dot{Z}_b \dot{Z}_L \dot{Z}_T \sigma_1}{4\dot{Z}_b \dot{Z}_T^3 \sigma_4 \sigma_3 \sigma_2} \\ \frac{V_i(2\dot{Z}_b \dot{Z}_T \sigma_0) + 2\dot{Z}_b \dot{Z}_L \dot{Z}_T \sigma_1}{4\dot{Z}_b \dot{Z}_T^3 \sigma_4 \sigma_3 \sigma_2} \\ \frac{-V_i \sigma_1}{2\dot{Z}_T \sigma_4 \sigma_3 \sigma_2} \\ \frac{V_i \sigma_1}{2\dot{Z}_T \sigma_4 \sigma_3 \sigma_2} \\ \frac{-V_i \sigma_0}{2\dot{Z}_b \dot{Z}_T \sigma_4 \sigma_3 \sigma_2} \\ \frac{2V_i \dot{Z}_T^2 (\sigma_4 \sigma_2 + \sigma_5 (\sigma_6 + \sigma_7 + 4\dot{Z}_b Z_{ES} \dot{Z}_L + 2\dot{Z}_b \dot{Z}_L \dot{Z}_T))}{2\dot{Z}_T \sigma_4 \sigma_3 \sigma_2} \\ \frac{V_i (\dot{Z}_T \sigma_4 \sigma_2 + \sigma_5 (\sigma_6 + \sigma_7 + 4\dot{Z}_b Z_{ES} \dot{Z}_L + 2\dot{Z}_b \dot{Z}_L \dot{Z}_T))}{\sigma_4 \sigma_3 \sigma_2} \\ \frac{V_i \sigma_5}{\sigma_2} \end{bmatrix}$$

$$\begin{aligned} \sigma_0 &= 2\dot{Z}_T^2 (\sigma_4 \sigma_2 + \sigma_5 (\sigma_6 + \sigma_7 + 4\dot{Z}_b Z_{ES} \dot{Z}_L + 2\dot{Z}_b \dot{Z}_L \dot{Z}_T)) \sigma_4 \\ &\quad - 4\dot{Z}_L \dot{Z}_T^3 (\sigma_4 \sigma_2 + \sigma_5 (\sigma_6 + \sigma_7 + 4\dot{Z}_b Z_{ES} \dot{Z}_L + 2\dot{Z}_b \dot{Z}_L \dot{Z}_T)); \\ \sigma_1 &= (2\dot{Z}_T (\sigma_4 \sigma_2 + \sigma_5 (\sigma_6 + \sigma_7 + 4\dot{Z}_b Z_{ES} \dot{Z}_L + 2\dot{Z}_b \dot{Z}_L \dot{Z}_T)) - 2\dot{Z}_T \sigma_5 \sigma_3) \sigma_4 \\ &\quad + 4\dot{Z}_T^3 (\sigma_4 \sigma_2 + \sigma_5 (\sigma_6 + \sigma_7 + 4\dot{Z}_b Z_{ES} \dot{Z}_L + 2\dot{Z}_b \dot{Z}_L \dot{Z}_T)); \\ \sigma_2 &= 8Z_{ES}^2 (\dot{Z}_L^2 + \dot{Z}_L \dot{Z}_T + \dot{Z}_b \dot{Z}_L + \dot{Z}_b \dot{Z}_T) + 4Z_{ES} \dot{Z}_L^2 (\dot{Z}_L + \dot{Z}_T + \dot{Z}_b) + \\ &\quad 4Z_{ES} \dot{Z}_T (\dot{Z}_L \dot{Z}_T + \dot{Z}_b \dot{Z}_L + \dot{Z}_b \dot{Z}_T) + 2\dot{Z}_L^2 \dot{Z}_T (\dot{Z}_L + \dot{Z}_b); \\ \sigma_3 &= \sigma_6 + \dot{Z}^2 + 2\dot{Z}_L \dot{Z}_T^2 + \sigma_7 + 4\dot{Z}_b Z_{ES} \dot{Z}_L + 4\dot{Z}_b Z_{ES} \dot{Z}_T + 2\dot{Z}_b \dot{Z}_L \dot{Z}_T + \\ &\quad 4Z_{ES} \dot{Z}_L \dot{Z}_T; \\ \sigma_4 &= 2\dot{Z}_b \dot{Z}_T + 2\dot{Z}_L \dot{Z}_T; \\ \sigma_6 &= 4Z_{ES} \dot{Z}_L^2; \\ \sigma_7 &= 2\dot{Z}_L^2 \dot{Z}_T; \end{aligned}$$

REFERENCES

[1] E. Jquier, and F. Constant, "Water as an essential nutrient: the physiological basis of hydration", *Eur. J. Clin. Nutr. vol., 64, no. 2, pp. 115-123, 2009*,
 [2] C. Tonozzi, E. Rudloff, and R. Kirby, "Perfusion versus hydration: impact on the fluid therapy plan," *Perfusion vol. 31, no. 12, 2009*.

[3] D. Pan, J. Han P. Wilburn, and S. G. Rockson, "Validation of a new technique for the quantitation of edema in the experimental setting," *Lymphat. Res. Biol.*, vol. 4 no. 3, pp.153-158, 2006.

[4] C. O'Brien, A. J. Young, and M. N. Sawka, "Bioelectrical impedance to estimate changes in hydration status," *Int. J. Sports Med.*, vol. 23 no. 5, pp. 361-366, 2002.

[5] L. E. Armstrong, A. C. Pumerantz, K. A. Fiala, M. W. Roti, S. A. Kavouras, D. J. Casa, and C. M. Maresh, "Human hydration indices: acute and longitudinal reference values," *Int. J. Sport Nutr. Exe.*, vol. 20 no. 2, pp.145-153, 2010.

[6] S. M. Shirreffs, "Markers of hydration status," *Eur. J. Clin. Nutr.*, vol. 57, S6-S9, 2003.

[7] S. Grimnes and . G. Martinsen, *Bioimpedance and Bioelectricity Basics*. London, U.K.: Academic, 2008.

[8] H. P. Schwan "Electrical properties of tissue and cell suspensions," *Adv. Biol. Med. Phys.*, vol. 5, pp.147-209, 1957.

[9] V. Nadda, J. Fialov, and J. Hercogov, "Management of lymphedema" *Dermatol. Ther.* vol. 25, no.4, pp.352-357, 2012.

[10] R. Xu, H. Zhu, and J. Yuan, "Electric-field intrabody communication channel modeling with finite-element method," *IEEE Trans. Biomed. Eng.*, vol. 58, no. 3 pp. 705-712, Mar. 2011.

[11] M. S. Wegmiller, A. Kuhn, J. Froehlich, M. Oberle, N. Felber, N. Kuster, and W. Fichtner, "An attempt to model the human body as a communication channel," *IEEE Trans. Biomed. Eng.*, vol. 54, no.10, pp. 1851-1857, Oct. 2007.

[12] K. Fujii, M. Takahashi, and K. Itao, "Electric field distributions of wearable devices using the human body as a transmission channel," *IEEE Trans. Antennas Propag.*, vol. 55, no.7, pp. 2080-2087, Jul. 2007.

[13] Y. Song, Q. Hao, K. Zhang, M. Wang, Y. Chu, and B. Kang, "The simulation method of the galvanic coupling intrabody communication with different signal transmission paths," *IEEE Trans. Instrum. Meas.*, vol. 60, no.4, pp. 1257-1266, Apr. 2011.

[14] B. Kibret, M. Seyedi, D. T. H.Lai, and M. Faulkner, "Investigation of Galvanic Coupled Intrabody Communication using Human Body Circuit Model," *IEEE J. Biomed. Health Inform.*, vol. 18 no. 4, pp. 1196-1206, 2014.

[15] S. H. Pun, Y. M. Gao, P. Mak, M. I. Vai, and M. Du, "Quasi-static modeling of human limb for intra-body communications with experiments," *IEEE Trans., Inf. Technol. Biomed.*, vol.15, no.6, pp. 870-876, Nov. 2011.

[16] P. O. Astrand and K. Rodahl, *Textbook of work Physiology, Physiological Bases of Exercise*, 3rd ed. New York: McGraw-Hill Book Company, 1986. pp. 412-485.

[17] D. Andreuccetti, R. Fossi, and C. Petrucci, *An Internet resource for the calculation of the dielectric properties of body tissues in the frequency range 10 Hz - 100 GHz*, Website at <http://niremf.ifac.cnr.it/tissprop/>. IFAC-CNR, Florence (Italy), 1997.

[18] M. S. Wegmueller, M. Oberle, N. Felber, N. Kuster, and W. Fichtner, "Signal transmission by galvanic coupling through the human body," *IEEE Trans. Instrum. Meas.*, vol. 59, no. 4, pp. 963969, Apr. 2010.

[19] M. S. Wegmueller, "Intra-body communication for biomedical sensor networks," Ph.D dissertation, ETH Zurich, Zurich, Switzerland, 2007.

[20] H. Skelton, "The storage of water by various tissues of the body," *Arch. Intern. Med.* vol. 40, no.2, pp. 140-152, 1927.

[21] A. Must and S. E. Anderson, "Body mass index in children and adolescents: considerations for population-based applications," *Int. J. Obes.*, Vol.30, pp.590-594, 2006.

[22] A. Ahlbom, U. Bergqvist, J. Bernhardt, J. Cesarini, M. Grandolfo, M. Hietanem, A. Mckinlay, R. Repacholi, D. Sliney, and J. Stolwijk, "Guidelines for limiting exposure to time-varying electric, magnetic, and electromagnetic fields (up to 300 GHz). International commission on non-ionizing radiation protection," *Health Phys.*, vol.74, no.4, pp. 494-522, Oct.1998.

[23] L. F. Fried and P. M. Palevsky, "Hyponatremia and hypernatremia," *Med. Clin. North Am.*, Vol.81, no.3, pp.585-609, 1997.

[24] W. Paul, "Energy expenditure and fat-free mass in men and women," *Am. J. Clin. Nutr.* Vol.34, no.9, pp. 1816-1826, 1981.

[25] Z. wang, P. Deurenberg, W. Wang, A. Pietrobelli, R. N. Baumgartner and S. B. Heymsfield, "Hydration of fat-free body mass: review and critique of a classic body-composition constant," *Am. J. Clin. Nutr.*, vol.69, no.5, pp. 833-841, 1999.

[26] M. D. Mifflin, S. T. St Jeor, L. A. Hill, B. J. Scott, S. A. Daugherty and Y.O. Koh, "A new predictive equation for resting energy expenditure in healthy individuals," *Am. J. Clin. Nutr.*, vol. 51, no.2, pp. 241-247, 1990.

[27] P. Ritz, G. Berrut, I. Tack, M. J. Arnaud and J. Tichet, "Influence of gender and body composition on hydration and body water spaces," *Clin. Nutr.*, vol.27, no.5, pp. 740-746, 2008.



Clement Ogugua Asogwa (M'09) received B.Eng degree in Electrical Engineering from University of Nigeria in 1999 and M.Eng degree in Information and Communication Engineering from Hunan University, Chnagsha China in 2012. He worked as Telecommunication Network and Implementation Engineer between 2000 and 2012. He is currently working towards his Phd degree at the College of Engineering and Science, Victoria University, Footscray Park, Melbourne, Australia. His research interests include signal processing and Intradody signal propagation for biomedical applications and sensors.



Assefa Teshome (M11) received the B.Sc. degree in Electrical Engineering from Bahir Dar University, Bahir Dar, Ethiopia in 2003; the M. Tech. degree in Electrical Engineering from Indian Institute of Technology – Madras (IIT–Madras), Chennai, India in 2007 and the M. Eng. (research) degree in Telecommunications engineering from the University of South Australia, Adelaide, Australia in 2013. He is currently working toward the Ph.D. degree in the College of Engineering and Science, Victoria University, Melbourne, Australia. His research interests include signal propagation and communication models for body area networks (BAN) in addition to signal processing techniques for Biomedical and Biometric applications.



Stephen Collins Stephen Collins obtained his BSc(Hons) and PhD in physics from the University of Melbourne. In 1986 he joined Victoria University and is a professor in the College of Engineering and Science. He has over 25 years of experience in research on optical fibre sensors including fluorescence-based temperature sensing and various aspects of fibre Bragg gratings used for sensing. He currently serves as the President of the Australian Optical Society and the Accreditation Manager of the Australian Institute of Physics.



Daniel Lai Daniel T.H. Lai received his B.Eng (Hons) and PhD degree in Electrical and Computer Systems from Monash University, Melbourne, Australia. He was a Postdoctoral Research Fellow in the University of Melbourne and Victoria University (2007-2010). He is currently with the College of Engineering and Science in Victoria University (2011). His research interests include computational modeling, sensors and communications for healthcare and sports applications. This involves the design of new non-invasive and proactive technologies capable of detecting, diagnosing and predicting health risks. He has over 100 peer-reviewed publications and is a current reviewer for several international journals e.g., IEEE Transactions of Information Technology and Biomedicine, Journal of Biomechanics and Sensors and Actuators. He is also actively involved in organization of several workshops and international conferences.